




Article

Assembly of Smart Microgels and Hybrid Microgels on Graphene Sheets for Catalytic Reduction of Nitroarenes

Muhammad Hashaam ¹, Sarmed Ali ^{2,*}, Tahreem Khan ¹, Muhammad Salman ¹, Shanza Rauf Khan ^{1,*}, Amjad Islam Aqib ³, Tean Zaheer ⁴, Shamsa Bibi ¹, Saba Jamil ¹, Merfat S. Al-Sharif ⁵, Samy F. Mahmoud ⁶ and Wangyuan Yao ^{7,8,*}

¹ Department of Chemistry, University of Agriculture, Faisalabad 38000, Pakistan

² Faculty of Engineering, Østfold University College, 1757 Halden, Norway

³ Department of Medicine, Cholistan University of Veterinary and Animal Sciences, Bahawalpur 63100, Pakistan

⁴ Department of Parasitology, University of Agriculture, Faisalabad 38040, Pakistan

⁵ Department of Chemistry, College of Science, Taif University, P.O. Box 11099, Taif 21944, Saudi Arabia

⁶ Department of Biotechnology, College of Science, Taif University, P.O. Box 11099, Taif 21944, Saudi Arabia

⁷ Department of Microbiology and Plant Pathology, University of California-Riverside, Riverside, CA 92521, USA

⁸ College of Veterinary Medicine, Huazhong Agricultural University, Wuhan 430070, China

* Correspondence: sarmedjutt@gmail.com (S.A.); shanza.khan@uaf.edu.pk (S.R.K.); wangyuay@ucr.edu (W.Y.)

Abstract: Poly (N-isopropylacrylamide-acrylic acid) [p(NIPAM-AAc)] microgel was successfully fabricated using the precipitation polymerization method. Silver (Ag) nanoparticles and graphene oxide (G) were used to fabricate the following hybrid microgels: Ag-p(NIPAM-AAc) (Ag-HMG), Ag-G-p(NIPAM-AAc) (Ag-G-HMG), and G-p(NIPAM-AAc) (G-HMG). Ag-HMG, Ag-G-HMG, and G-HMG were characterized using a Zetasizer and UV-Vis spectroscopy. The reduction of a series of different compounds with comparable and distinct chemical structures was catalyzed by synthesized Ag-HMG, Ag-G-HMG, and G-HMG hybrid microgels. The average size of Ag nanoparticles was found to be ~50 nm. Ag nanoparticles were synthesized within microgels attached to G sheets. Ag-p(NIPAM-AAc), Ag-G-p(NIPAM-AAc), and G-p(NIPAM-AAc) hybrid microgels were used for the catalytic reduction of nitroarenes and dyes. By comparing their apparent rate constant (k_{app}), reduction duration, and percentage reduction, the activity of HMG (hybrid microgel) as a catalyst towards different substrates was investigated. Graphene sheets play role in electron relay among Ag nanoparticles and microgels.

Keywords: microgel; nanoparticles; silver; graphene; reduction



Citation: Hashaam, M.; Ali, S.; Khan, T.; Salman, M.; Khan, S.R.; Aqib, A.I.; Zaheer, T.; Bibi, S.; Jamil, S.; Al-Sharif, M.S.; et al. Assembly of Smart Microgels and Hybrid Microgels on Graphene Sheets for Catalytic Reduction of Nitroarenes. *Catalysts* **2022**, *12*, 1172. <https://doi.org/10.3390/catal12101172>

Academic Editor: Lihua Bi

Received: 20 August 2022

Accepted: 25 September 2022

Published: 5 October 2022

Publisher's Note: MDPI stays neutral with regard to jurisdictional claims in published maps and institutional affiliations.



Copyright: © 2022 by the authors. Licensee MDPI, Basel, Switzerland. This article is an open access article distributed under the terms and conditions of the Creative Commons Attribution (CC BY) license (<https://creativecommons.org/licenses/by/4.0/>).

1. Introduction

Microgels are distinct gel particles with a size in the colloidal range of 5–500 nm and are composed of crosslinked polymer chains, which is a typical internal arrangement of polymer networks [1]. Nanoparticles containing microgels are called hybrid microgels (HMGs) [2]. Microgels act as stabilizing agents and inhibit the aggregation of nanoparticles [3,4]. This type of hybrid material possesses the exceptional properties of both microgels and metal nanoparticles [5]. The synthesis and characterization of microgels containing temperature-responsive polymers have attracted more attention in recent years. HMG is a material that has the strength, conductivity, and photosensitivity properties of nanoparticles and the viscoelasticity of polymers [6].

HMGs (polymer microgels produced with inorganic nanoparticles) have received a lot of attention as catalytic devices for reducing toxic chemicals [7]. Nitro arenes and organic dyes are toxic chemicals [8,9]. Their degradation or reduction is very slow in the environment [10]. The accumulation of these compounds in water bodies is increasing day

by day [11], so efficient methods of removing these substances have been researched. It is better to convert these toxic compounds into useful compounds, such as amino arenes. Das et al. have synthesized silver (Ag) nanoparticles illuminated cerium oxide nanotubes catalyst for the reduction of 4-nitrophenol (4-NP) [12]. Das et al. have also tried to modulate the catalytic reduction of 4-NP using thermoresponsive Ag nanoparticles entrapped in resin nanocomposite as a catalyst [13]. Jamil et al. have reported the catalytic reduction of dyes using nickel oxide/polyaniline nanocomposite as a catalyst [14].

The improved catalytic behavior of HMGs is linked to the sensitive nature of microgels to a specific stimulus and the exceptional stability of nanoparticles inside the network of polymer microgels. The catalytic properties of HMGs can be easily tuned through slight changes in ambient conditions. In the presence of an HMG catalytic system, the catalytic reduction of nitroarenes and organic dyes has been explained [15]. Smart polymer microgels loaded with metal sulfide [16], metal oxide [17], and metal nanoparticles [18] have been used as catalysts in the reduction of nitroarenes and organic dyes. In these HMGs, metal nanoparticle-loaded microgels have often been used [19].

Graphene is a two-dimensional material [20] that possesses a single layer of sp^2 hybridized carbon atoms [21], and it is the thinnest and hardest material [22]. Graphene shows distinct characteristics, including a large surface area, high charge carrier mobility, and high thermal conductivity [23], which ensure its high catalytic activity. The addition of metal oxide nanoparticles to graphene reduces aggregation, thus resulting in the increased surface area of the composite [24]. Graphene permits the electrons to bounce among microgel particles. The potential of graphene as an adsorbent to remove various dyes, heavy metal ions, and other aromatic pollutants has been studied [25]. Aside from pure graphene, surfactant-modified graphene, nanomaterials, polymers, and biomolecules have been investigated as adsorbents and observed to have high adsorption efficiency. The active groups, such as carbonyl, epoxy, and hydroxyl groups, present on the surface of graphene oxides allow it to interact with a wide range of molecules and thus undergo surface modification [26]. Furthermore, through surface complexation, these entangled active groups of graphene oxide can connect to heavy metal ions present in the solution, allowing it to be utilized to extract ions from the solution [27]. It was previously reported that graphene oxide/poly(N-isopropylacrylamide) (GO/PNIPAM) hybrid microgel was used to purify water from toxic dyes and contaminants [28], and the reduction of organic pollutants, such as Congo red, 4-nitroanisole (4-NA), methylene orange, 4-nitrophenol (4-NP), methylene blue, Safranin, 2,4 dinitrophenol (2,4-DNP), and 4-nitrobenzoic acid (4-NBA), using zirconium-poly(N-isopropylacrylamide-methacrylic acid)@graphene composite as a catalyst was reported [29].

As low-cost catalysts for the reduction of nitroarenes and organic dyes, Ag nanoparticles synthesized as smart microgels have gained interest [30,31]. The most common method for producing and stabilizing Ag nanoparticles is to reduce the silver ions within polymer microgels with a suitable reducing agent [32]. The ease of availability of salt precursors—polymer microgels loaded with Ag nanoparticles—has attracted a lot of attention in comparison to other noble metal salts, such as gold (Au), platinum (Pt), and palladium (Pd) [33]. Zhang et al. developed poly(N-isopropylacrylamide-maleated carboxymethylchitosan) [p(NIPAM/MACS)]-responsive microgels through co-precipitation polymerization loaded with Ag nanoparticles to explore the catalytic behavior for the reduction of nitroarenes [34]. For the reduction of 4-nitrophenol via $NaBH_4$, the hybrid system showed strong catalytic activity. Lu et al. described the production of poly(styrene)-p(N-isopropylacrylamide)-silver (PS-PNA-Ag) core-shell HMG and investigated their catalytic potential [35]. Small and uniform-sized Ag nanoparticles were successfully produced in the shell region of core-shell microgels, with catalytic efficiency proportional to the surface area of the silver nanoparticles [36]. Shah et al. developed a stimuli-responsive homogeneous microgel system with Ag nanoparticles and investigated its catalytic activity for methylene blue reduction in an aqueous medium [37]. Simple free radical precipitation polymerization was used to make P(NIPAM) microgels, and Ag nanoparticles were produced within the

polymer microgels through in situ reductions of Ag ions. Khan et al. developed an Ag-poly [N-isopropylacrylamide-co-allyl acetic acid] hybrid catalytic system for nitrobenzene reduction. The effect of NaBH₄ and catalyst dosage on nitrobenzene reduction rate constant values was examined. The study concluded that the Langmuir–Hinshelwood mechanism operates after catalytic reduction [38].

Nitroarenes are highly toxic and harmful to the environment [39] and are widely used in sectors such as explosives [40], medicines [41], and textiles [15]. Nitroarenes are commonly utilized as precursors in the production of insecticides, pharmaceuticals, and colors [42]. Dyes are a type of organic substance that is often utilized in the textile [43], cosmetic [44], and chemical industries [45]. During the dyeing process, over 15% of the total dye output is wasted. The reduction of organic waste, including nitroarenes and organic dyes, is becoming increasingly important as a result of these factors. These pollutants can be converted into less harmful substances using various methods, such as catalytic reduction, hydrogenation, degradation, and physical adsorption [46]. Catalytic reduction is the most widely used method for the reduction of nitroarenes [47–49].

The present research work involved the synthesis of Ag-p(NIPAM-AAc), G-p(NIPAM-AAc), and Ag-G-p(NIPAM-AAc) hybrid microgels through the polymerization precipitation method. The synthesized hybrid microgels were characterized using Zetasizer and UV-Vis spectroscopy. A Zetasizer was used for the measurement of particle size and polydispersity index of Ag-HMG, Ag-G-HMG, and G-HMG hybrid microgels. The purpose of this study was to compare the catalytic efficiency of Ag-p(NIPAM-AAc), G-p(NIPAM-AAc), and Ag-G-p(NIPAM-AAc) hybrid microgels in the reduction of organic compounds, such as dyes and nitroarenes. The comparison of k_{app} , reduction time, and reduction percentage are also discussed.

2. Results and Discussion

2.1. Zeta Potential Analysis of Hybrid Microgels

A zeta analysis was used to determine the size and size distribution of the samples. The results of the DLS Zetasizer show the zeta potential measurements of Ag-HMG, Ag-G-HMG, and G-HMG. Three bands were observed in the plot of Ag-HMG hybrid microgel shown in Figure 1. These three bands were centered on 5, 50, and 5200 nm. The band around 50 nm indicated the size of the Ag-HMG hybrid microgel, which correlates to the STEM analysis results (Figure S1). The band around 5 nm predicted that the size was very small, which could be the size of Ag nanoparticles present outside the microgel. The band around 5200 nm showed that the Ag-HMG hybrid microgel was aggregated, which refers to the presence of Ag nanoparticles between the microgel. Ag-HMG with an average particle size of 50 nm has a very uniform distribution, which can be observed when peaks with an intensity of 92.5% appear. The first small peak showed that some Ag nanoparticles were in the range of 5–10 nm; these nanoparticles are not inside the microgel system shown in Figure 1. This refers to the monodispersity of the nanoparticles, which makes the nanoparticles very stable for a long time. In addition, the (PDI) was 0.385, indicating that the formed Ag nanoparticles had high stability and homogeneity.

Two bands were observed in the plot of Ag-G-HMG hybrid microgel. These two bands were centered on 160 and 1740 nm. The band around 160 nm indicated that the hybrid microgel overlapped with each other. The band around 1740 nm predicted that particles of the hybrid microgel (Ag-G-HMG) were fabricated on the graphene sheets. These two peaks in Ag-G-HMG showed the size distribution analysis, showing more than 80% of nanoparticles in the system were around 160 nm, which indicated that gel particles appeared fused. Their boundaries were joined with each other, whereas the PDI of 0.509 indicated that Ag-G-HMG was less monodisperse in comparison with Ag-HMG. Similarly, two bands were observed in the plot of G-HMG. These two bands were centered on 550 and 4480 nm. These two peaks possessed intensity levels of 88.9 and 11.1, respectively. The size distribution analysis of the G-HMG hybrid microgel revealed a sharp, strong, and intense peak, showing more than 90% of particles in the system were around

550 nm, which indicates that gel particles were fabricated on graphene sheets, whereas a PDI of 0.482 indicated that G-HMG was less monodisperse compared to Ag-HMG but a slightly good result in comparison with Ag-G-HMG.

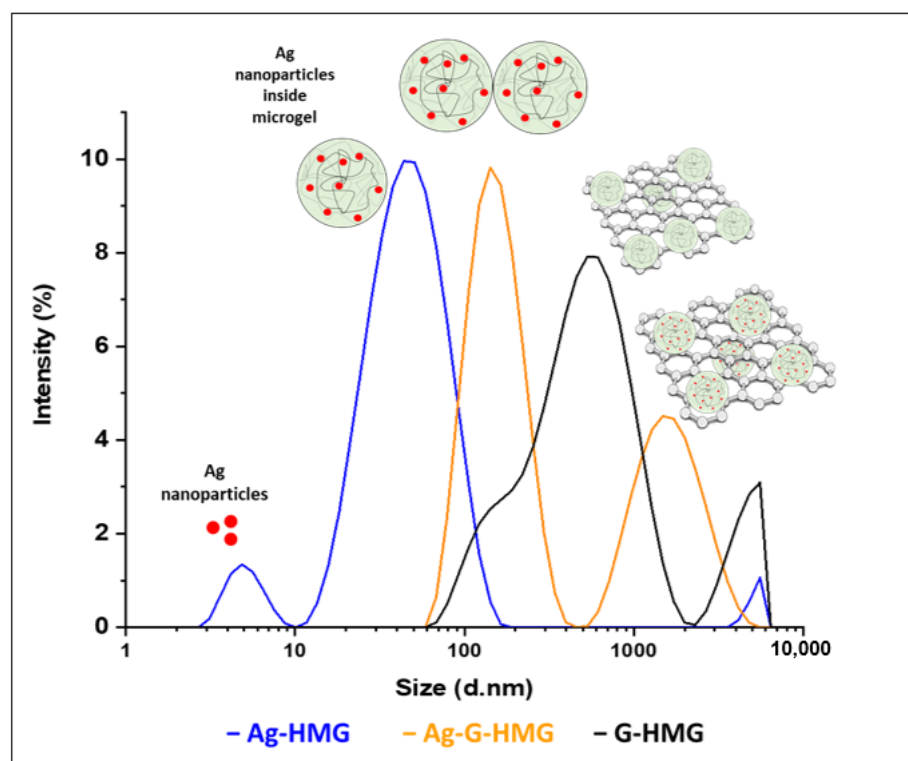


Figure 1. Zeta potential analysis of hybrid microgels.

2.2. Catalytic Applications of Hybrid Microgels

The catalytic reduction of dyes and nitroarenes using hybrid microgels as catalysts and NaBH_4 as a reducing agent was investigated. The time-dependent plot of the catalytic reduction of nitroarenes (4-NP, 4NAs, 2,4 DNP) and dyes (RB-5, MG, MR, EBT, and MO) is shown in Figure 2. The organic compounds, such as MR, RB-5, MG, EBT, MO, 4-NP, 4-NAs, and 2,4 DNP, showed maximum absorbance at 430, 595, 617, 530, 500, 400, 320, and 360 nm, respectively. NaBH_4 was used, in excess quantity, as the concentration of substrate. The dynamics of this reduction were pseudo-first-order, as the pH of the reaction medium was above 10. Carboxyl groups of AAc were ionized at this pH because the medium pH was greater than the pK_a of AAc [50]. Due to repulsion among carboxyl groups, hybrid microgel sieves were opened and molecules of 4-NP, 4NAs, 2,4 DNP, and NaBH_4 were easily fluxed through the sieve and adsorbed on the active surfaces. Ag nanoparticles served as a route for electron density transfer from BH_4^- to 4-NP, 4NAs, and 2,4 DNP. The transfer of electron density from BH_4^- to organic azo dye was also enhanced by Ag nanoparticles. The cleavage of the azo link is required for the catalytic reduction of organic dyes.

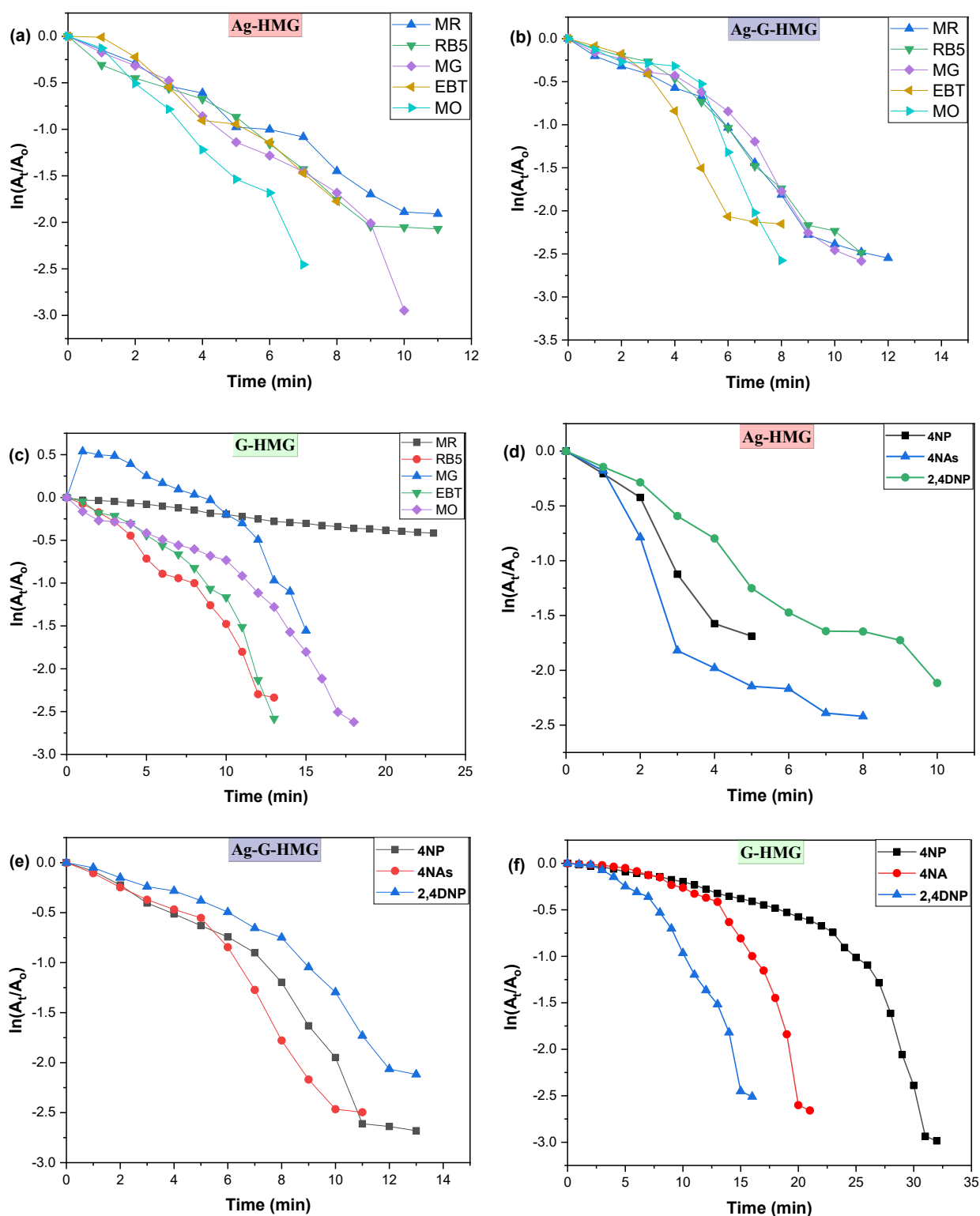


Figure 2. A plot of $\ln(A_t/A_0)$ versus time of catalytic reduction of MR, RB-5, MG, EBT, MO using (a) Ag-HMG, (b) Ag-G-HMG, and (c) G-HMG as catalysts and a plot of $\ln(A_t/A_0)$ versus time of catalytic the reduction of 4-NP, 4-NAs, and 2,4 DNP using (d) Ag-HMG, (e) Ag-G-HMG, and (f) G-HMG as catalysts.

2.2.1. Comparison of k_{app} of Dyes and Nitro Compounds

Figure 3 provides a comparison of the k_{app} of different substrates reduced through the use of Ag-HMG, G-Ag-HMG, and G-HMG as catalysts. k_{app} values of the nitro compounds

are shown to be higher compared to the k_{app} value of organic dyes. Ag-HMG, G-Ag-HMG, and G-HMG hybrid microgel catalysts that possess binding inside the microgel network accessibility of 4-NAs were higher than other nitro compounds. BH_4^- easily reduced the nitro-group into the amino groups as compared with the substrate. The reduction of 4-NAs was the maximum among all other substrates. The plot shows that the k_{app} value of 4-NAs was at the maximum. The existence of open-positioned MeO groups (methoxy groups) and nitro bulky groups in 4-NAs accelerated nitro-bond reduction. The 4-NAs positively charged nitrogen atom was extremely electrophilic, favoring a BH_4^- -mediated nucleophilic attack. When the k_{app} values are compared, it can be seen that nitrophenols reduce faster than azo dyes. The 4-NAs and MO are slightly more highly reducible compared to the other organic pollutants. The catalytic reduction of 4-NAs and MO was greater than other compounds due to the rapid transfer of electron density on the active sites of Ag-HMG and Ag-G-HMG, respectively, as compared to other organic pollutants. The rate of catalytic reduction of organic dyes depends on the bulkiness of the aromatic rings around the azo group of dye. MO and EBT were significantly reduced due to less bulkiness and the easy cleavage of the azo group. High stability in the structure of MR restricted the cleavage of the azo group. Therefore, MR showed the lowest k_{app} value compared to other substrates.

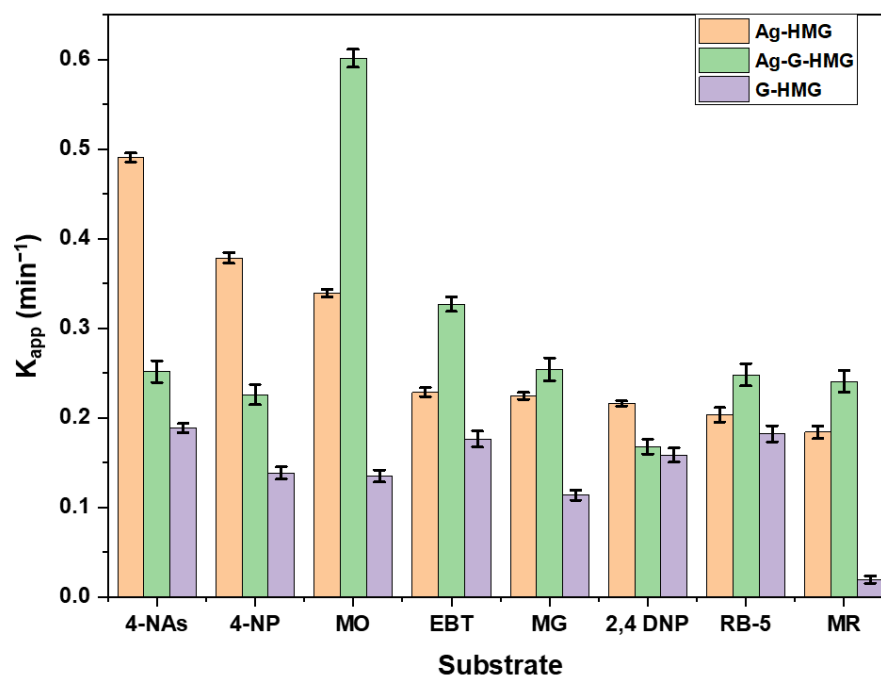


Figure 3. A plot of comparisons of the k_{app} of different substrates reduced through the use of different hybrid microgels as catalysts.

2.2.2. Comparison of Reduction Time

The reduction time comparison of different substrates between Ag-HMG, G-Ag-HMG, and G-HMG catalysts is shown in Figure 4. The plot showed that the reduction time of MR was higher in comparison with other compounds. The 4-NP reduction time was the lowest because of the presence of fewer bulky aromatic rings around the azo group. More time of contact of the nitroarenes, maximum flux, and maximum adsorption with Ag-HMG, Ag-G-HMG, and G-HMG hybrid microgels increased the rate of reduction of the nitro-compounds compared to azo dyes. In comparison to other substrates, 4-NP was reduced in a shorter amount of time, as shown in the graph. However, for the Ag-G-HMG hybrid microgel, 4-NP showed a high reduction time due to the electrostatic interaction between COO^- of the Ag-G-HMG hybrid microgel network and 4-NP. The removal of bulky groups (less hindrance) contributed to the rapid reduction of MO. Among all the substrates, 4-NP had the quickest reduction time. The similarity between the structures of

the MR and RB-5 bulk azo groups attached in their structures showed a similar trend in reduction time in the existence of different HMG, with a slight deviation.

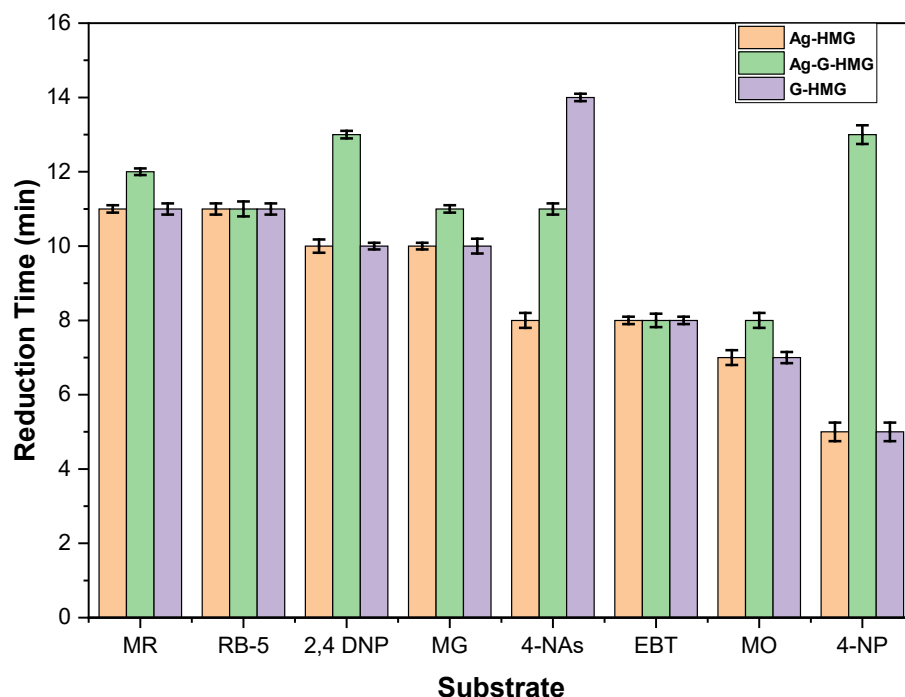


Figure 4. A plot of comparisons of the reduction times of different substrates reduced through the use of different hybrid microgels as catalysts.

2.2.3. Comparison of Percentage Reduction

Figure 5 plot provides a comparison of the percentage reductions for different substrates using Ag-HMG, G-Ag-HMG, and G-HMG as catalysts. The reduction of a substrate depended on structure similarity, the orientation of the functional group, and the nature of bond breakdown during the transformation of electron density. MG, MO, 4-Nas, and other compounds were maximally reduced due to the high recognition ability and similarity between the structures of the synthesized hybrid microgels (Ag-HMG, G-Ag-HMG). The high reduction percentage of MO was due to the similarity between the structures of MG, as compared to 2,4 DNP, RB-5, MR, and EBT. Ag-HMG, G-Ag-HMG, and G-HMG were easily recognized by MG as compared with other substrates. The presence of bulky aromatic rings around the azo group hindered the cleavage of the azo group, which may have reduced the reduction percentage of the substrate. The increase in the specific surface or surface/volume ratio of Ag-HMG could be the reason for its excellent catalytic activity in reducing organic dyes. MR was not significantly reduced due to high structure stability, as compared to other substrates. MR showed the lowest reduction percentage, and 4-NP showed the highest reduction percentage with G-HMG, as shown in Figure 5.

A summary of the reduced concentrations of different substrates is provided in Table 1. The N-group (the group containing nitro) was reduced into the A-group (the group containing amino), and the A-group was reduced into N–N in the excess presence of NaBH₄ using a synthesized catalyst (Ag-HMG, Ag-G-HMG, and G-HMG), which resulted in reduced (colorless) compounds. C_i , C_f , and C_r concentration details are also shown. Substrates were reduced into 4-AP, 2,4-DAP, 4AAS, and other amino compounds. The synthesized G-HMG catalyst showed a maximum reduction of different substrates as compared to Ag-HMG and Ag-G-HMG.

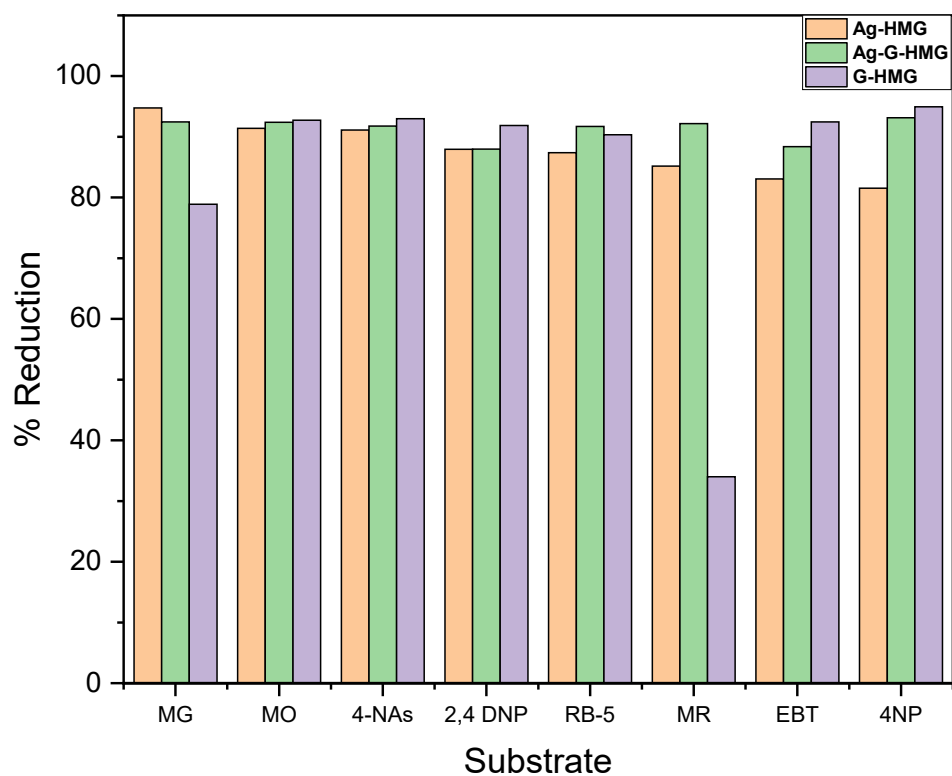
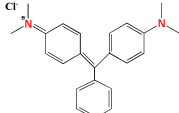
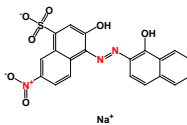
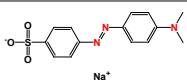


Figure 5. A plot of comparisons of the reduction percentages of different substrates reduced through the use of different hybrid microgels as catalysts.

Table 1. Comparison of initial, final, reduced concentrations and reduction time of substrates using Ag-HMG, Ag-G-HMG, and G-HMG hybrid microgels, respectively, as catalysts.

Substrate	Ag-HMG			Ag-G-HMG		G-HMG	
	Initial Concentration (mM)	Final Concentration (mM)	Reduced Concentration (mM)	Final Concentration (mM)	Reduced Concentration (mM)	Final Concentration (mM)	Reduced Concentration (mM)
4-NP 	0.1	0.019	0.081	0.007	0.093	0.005	0.095
4-NAs 	0.1	0.009	0.091	0.008	0.092	0.007	0.093
2,4 DNP 	0.1	0.012	0.088	0.012	0.088	0.008	0.092
MR 	0.1	0.0155	0.0845	0.008	0.092	0.067	0.033
RB-5 	0.1	0.013	0.087	0.009	0.091	0.009	0.091

Table 1. Cont.

Substrate	Ag-HMG			Ag-G-HMG		G-HMG	
	Initial Concentration (mM)	Final Concentration (mM)	Reduced Concentration (mM)	Final Concentration (mM)	Reduced Concentration (mM)	Final Concentration (mM)	Reduced Concentration (mM)
MG 	0.1	0.005	0.095	0.008	0.092	0.021	0.079
EBT 	0.1	0.017	0.083	0.012	0.088	0.007	0.093
MO 	0.1	0.009	0.091	0.008	0.092	0.007	0.093

2.2.4. Comparison of Stability

The stability of the Ag-HMG, Ag-G-HMG, and G-HMG catalysts has been studied using 4-NP as a substrate. The stability of the catalysts was studied in terms of their percentage of efficiency. All the catalysts were found to be stable over four cycles (Figure 6). Little decrease in catalytic activity was observed. The general percentage of efficiency trend was AG-G-HMG > G-HMG > Ag-HMG. Graphene provided mechanical strength to microgels, so the stability of G-HMG and Ag-G-HMG catalysts was high. The oxide layer was formed around Ag nanoparticles when used in an aqueous medium, so its percentage of efficiency was decreased after every cycle [51].

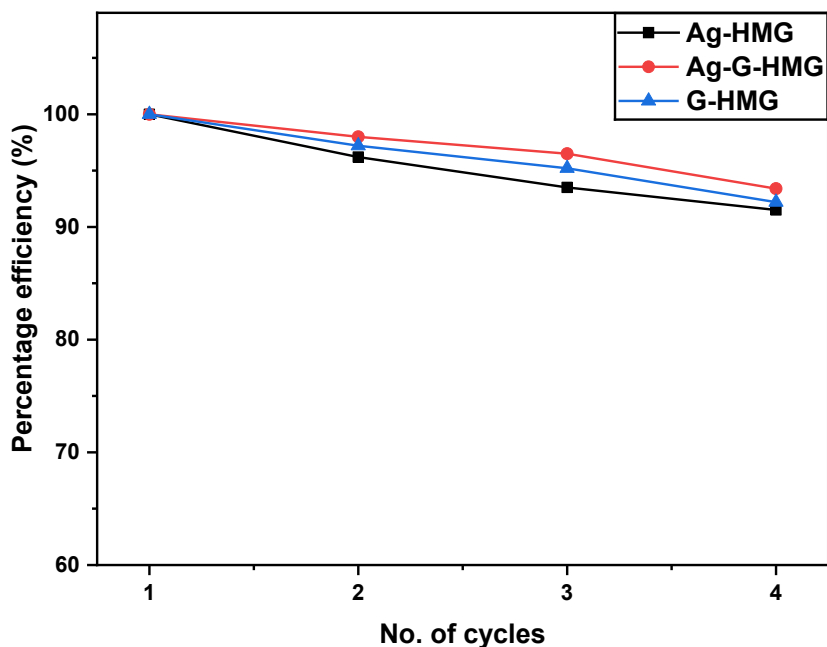


Figure 6. Percentage of efficiency of catalysts as a function of the number of cycles.

3. Experimental

3.1. Materials

N-isopropyl acrylamide ($C_6H_{11}NO$)_n, Sodium Dodecyl Sulfate (SDS), Ammonium persulfate (APS), N,N methylenebisacrylamide (BIS), Silver nitrate ($AgNO_3$), Sodium hydroxide (NaOH), Sodium borohydride ($NaBH_4$), Polyvinylpyrrolidone (PVP), 4-Nitrophenol ($C_6H_5NO_3$), 4-Nitroanisole ($C_7H_5NO_3$), 2,4-Dinitrophenol ($C_6H_4N_2O_5$), Methyl red ($C_{15}H_{15}N_3O_2$), Re-

active black-5 ($C_{26}H_{21}N_5Na_4O_{19}S_{16}$), Malachite green ($C_{23}H_{25}N_2$), Eriochrome black-T ($C_{20}H_{12}N_3O_7SNa$), and Methyl orange ($C_{14}H_{14}N_3NaO_3S$) were purchased from Sigma-Aldrich, Louis, MO, USA. All of the chemical compounds were of analytical grade and used without any purification. Fresh distilled water was used to make all of the solutions.

3.2. Synthesis of *p*(NIPAM-Acrylic Acid) Microgel

The precipitation polymerization (PP) method was used to make *p*(NIPAM-AAc), and 0.92 g of NIPAM, 0.04 mL of AAc, and 0.07 g of BIS were dissolved in 95 mL of distilled water in a round bottom flask. In the resulting solution, 0.05 g of surfactant (SDS) was dissolved and agitated for 30 min at 70 °C. Then, 5 mL of APS (0.05 M) was added and agitated continuously for 5 h at 70 °C. Molecular porous membrane tubing was used to dialyze synthesized *p*(NIPAM-AAc) against distilled water for a week at room temperature. The whole process is drawn schematically in Figure 7.

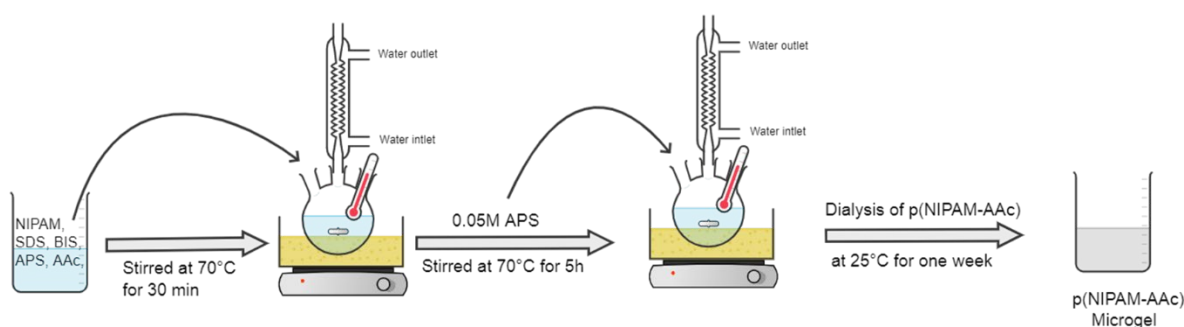


Figure 7. Schematic diagram of the synthesis of *p*(NIPAM-AAc) microgels.

3.3. Synthesis of Graphene

Graphene was synthesized using the Hummers method [52]. We used the same graphene that was already prepared and explained in our paper: Ali et al. [29]. The schematic diagram of the synthesis of graphene is provided below in Figure 8.

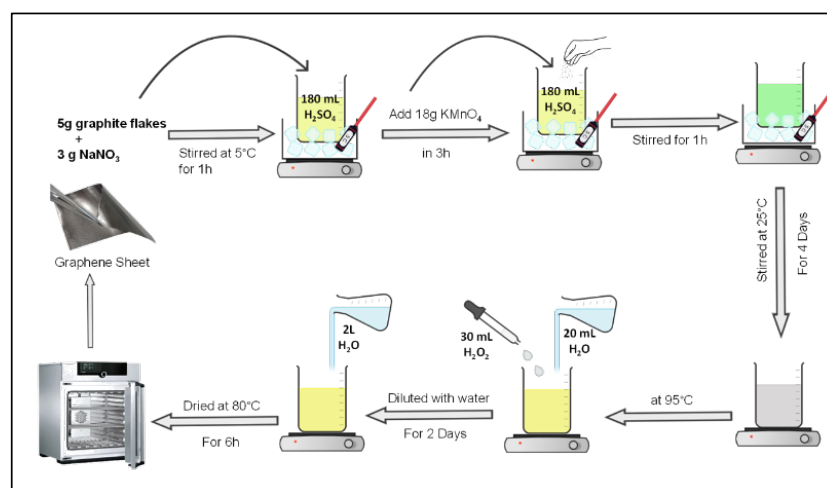


Figure 8. Schematic diagram of the synthesis of graphene using Hummer's method.

3.4. Synthesis of Hybrid Microgels

HMG embedded with Ag nanoparticles was prepared using the in situ chemical reduction method (Figure 9) [53]. In a round-bottom flask, 20 mL *p*(NIPAM-AAc) dispersion of microgel and 14 mL of H_2O were added and stirred for 30 min at a pH of 9. To keep the pH at 9, NaOH was utilized. In the microgel dispersion, 1.8 mL of $AgNO_3$, having a molar concentration of 0.01 M, was added and agitated for 30 min at room temperature.

The reaction mixture was then agitated for another 60 min after adding 0.02 g of NaBH_4 . A semipermeable membrane was used to dialyze an Ag-p(NIPAM-AAc) hybrid microgel against pure water. After that, the obtained product was divided into two equal portions.

Next, 0.3 g of powdered graphene was added to one portion of Ag-p(NIPAM-AAc), and the reaction mixture was stirred for 2 h at room temperature in the round-bottom flask. An Ag-G-p(NIPAM-AAc) hybrid microgel was obtained at the end of the reaction.

Then, 10 mL of synthesized p(NIPAM-AAc) microgel and 7 mL of distilled water were added into a round-bottom flask and stirred for 30 min at a pH of 9 to synthesize hybrid microgel G-p(NIPAM-AAc). NaOH was used to maintain a pH of 9, and 0.3 g of powdered graphene was mixed into the medium and stirred for 2 h at room temperature in the round-bottom flask.

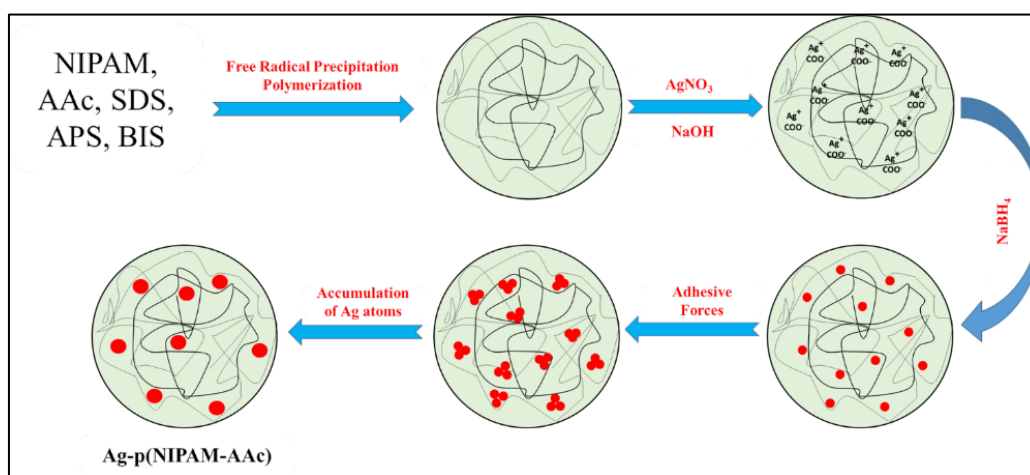


Figure 9. Diagrammatic representation of the synthesis of Ag nanoparticles within p(NIPAM-AAc) HMGs through in situ reaction.

3.5. Catalytic Application

Organic compounds, i.e., MO, MR, MG, RB-5, EBT, 4-NP, 4-NAs, and 2,4-DNP, were used as substrates to compare the catalytic activity of synthesized products, i.e., Ag-HMG, G-HMG, and Ag-G-HMG hybrid microgels. λ_{max} of EBT, MO, 4-NP, RB-5, MR, MG, and 2,4-DNP in an aqueous medium was observed as 530, 500, 400, 595, 430, 617, and 360 nm, respectively. A total of 3 mL of 0.1 mM solution of organic compounds, 0.5 mL of hybrid microgel, and 0.01 g of NaBH_4 were added into a cuvette and placed in a UV-Vis spectrophotometer to examine the progress of the catalytic reduction. The absorbance of the solution was observed at different intervals of time at λ_{max} .

3.6. Characterization

The measurement of particle size and polydispersity index of Ag-HMG, Ag-G-HMG, and G-HMG via Zetasizer (ver. 7.11; serial number: MAL1127001, Malvern Zen 3600, Malvern Panalytical, Malvern, UK), which was available from the National Textile University, Faisalabad. A BMS VIS-1100 spectrophotometer (Bristol Myers Squibb, New York, NY, USA), used for UV-Vis spectrophotometry, was obtained from the Postgraduate Agricultural Research Station (PARS), University of Agriculture, Faisalabad.

4. Conclusions

P(NIPAM-AAc) microgel was successfully synthesized through precipitation polymerization with a free radical mechanism, graphene was synthesized using Hummer's method, and Ag nanoparticles were manufactured via the in situ chemical reduction method. The size range of fabricated Ag nanoparticles was 5–50 nm. Azo dyes and nitroarenes were reduced through the use of synthesized hybrid microgels as catalysts. In this research work, we described the synthesis of Ag nanoparticles fabricated from

poly(*N*-isopropylacrylamide-co-acrylic acid) hybrid microgel—Ag-p(NIPAM-AAc), Ag-G-p(NIPAM-AAc), and G-p(NIPAM-AAc) hybrid-microgels—that were used for the reduction of different organic compounds (4-NP, 4-NAs, 2,4 DNP, RB-5, EBT, MG, MO, and MR). Prepared HMGs were characterized using a Zetasizer and UV-Vis spectroscopy. The monodispersity of fabricated Ag nanoparticles was confirmed by a sharp absorption band and low PDI (0.385), as observed with a Zetasizer. The reduction of substrates was dependent upon the Langmuir–Hinshelwood mechanism. The k_{app} values, the reduction percentage, and the reduction time of substrates, using the synthesized hybrid microgels, were studied. The k_{app} value, the reduction percentage, and the reduction time of 4-NP were observed as being higher as compared to other substrates.

Supplementary Materials: The following supporting information can be downloaded at: <https://www.mdpi.com/article/10.3390/catal12101172/s1>, Figure S1: STEM analysis of Ag-HMG microgels.

Author Contributions: Conceptualization, S.A. and S.R.K.; data curation, A.I.A. and S.B.; formal analysis, S.A. and A.I.A.; investigation, T.K. and M.S.; methodology, M.H. and T.K.; project administration, S.R.K.; resources, M.S.A.-S., S.F.M. and W.Y.; Supervision, A.I.A.; validation, T.Z. and S.J.; visualization, M.S., S.F.M. and T.Z.; writing—original draft, M.H.; Writing—review and editing, M.S.A.-S., S.F.M. and W.Y. All authors have read and agreed to the published version of the manuscript.

Funding: This research received no external funding.

Data Availability Statement: Not applicable.

Acknowledgments: Authors wish to acknowledge the Taif University Researchers Supporting Project number (TURSP-2020/138), Taif University, Taif, Saudi Arabia for financial support. The authors are highly thankful to UAF Community College and Department of Chemistry, University of Agriculture, Faisalabad 38000, Pakistan for support and financial assistance.

Conflicts of Interest: The authors declare no conflict of interest.

References

1. Prashant, P.; Seo, S.S. Organophosphate Nerve Agent Sensor Based on Polystyrene Core and Zirconium Shell Colloidal Crystal Array. *Int. J. Polym. Anal. Charact.* **2009**, *14*, 481–492. [CrossRef]
2. Karg, M.; Hellweg, T. Smart inorganic/organic hybrid microgels: Synthesis and characterisation. *J. Mater. Chem.* **2009**, *19*, 8714–8727. [CrossRef]
3. Brugger, B.; Richtering, W. Emulsions stabilized by stimuli-sensitive poly (*N*-isopropylacrylamide)-co-methacrylic acid polymers: Microgels versus low molecular weight polymers. *Langmuir* **2008**, *24*, 7769–7777. [CrossRef]
4. Khan, A.; El-Toni, A.M.; Alrokayan, S.; Alsalhi, M.; Alhoshan, M.; Aldwayyan, A.S. Microwave-assisted synthesis of silver nanoparticles using poly-*N*-isopropylacrylamide/acrylic acid microgel particles. *Colloids Surf. A* **2011**, *377*, 356–360. [CrossRef]
5. Liu, Y.-Y.; Liu, X.-Y.; Yang, J.-M.; Lin, D.-L.; Chen, X.; Zha, L.-S. Investigation of Ag nanoparticles loading temperature responsive hybrid microgels and their temperature controlled catalytic activity. *Colloids Surf. A Physicochem. Eng. Asp.* **2012**, *393*, 105–110. [CrossRef]
6. Plamper, F.A.; Richtering, W. Functional microgels and microgel systems. *Acc. Chem. Res.* **2017**, *50*, 131–140. [CrossRef] [PubMed]
7. Echeverria, C.; Fernandes, S.N.; Godinho, M.H.; Borges, J.P.; Soares, P.I. Functional stimuli-responsive gels: Hydrogels and microgels. *Gels* **2018**, *4*, 54. [CrossRef]
8. Das, T.K.; Das, N.C. Advances on catalytic reduction of 4-nitrophenol by nanostructured materials as benchmark reaction. *Int. Nano Lett.* **2022**, *12*, 223–242. [CrossRef]
9. Singh, S.; Rao, C.; Nandi, C.K.; Mukherjee, T.K. Quantum Dot-Embedded Hybrid Photocatalytic Nanoreactors for Visible Light Photocatalysis and Dye Degradation. *ACS Appl. Nano Mater.* **2022**, *5*, 7427–7439. [CrossRef]
10. Naz, M.; Rafiq, A.; Ikram, M.; Haider, A.; Ahmad, S.O.A.; Haider, J.; Naz, S. Elimination of dyes by catalytic reduction in the absence of light: A review. *J. Mater. Sci.* **2021**, *56*, 15572–15608. [CrossRef]
11. Mejía, Y.R.; Bogireddy, N.K.R. Reduction of 4-nitrophenol using green-fabricated metal nanoparticles. *RSC Adv.* **2022**, *12*, 18661–18675. [CrossRef]
12. Das, T.K.; Remanan, S.; Ghosh, S.; Ghosh, S.K.; Das, N.C. Efficient synthesis of catalytic active silver nanoparticles illuminated cerium oxide nanotube: A mussel inspired approach, Environmental Nanotechnology. *Monit. Manag.* **2021**, *15*, 100411. [CrossRef]
13. Kanti Das, T.; Ganguly, S.; Remanan, S.; Das, N.C. Temperature-Dependent Study of Catalytic Ag Nanoparticles Entrapped Resin Nanocomposite towards Reduction of 4-Nitrophenol. *ChemistrySelect* **2019**, *4*, 3665–3671. [CrossRef]
14. Jamil, S.; Ahmad, Z.; Ali, M.; Khan, S.R.; Ali, S.; Hammami, M.A.; Haroon, M.; Saleh, T.A. Synthesis and characterization of polyaniline/nickel oxide composites for fuel additive and dyes reduction. *Chem. Phys. Lett.* **2021**, *776*, 138713. [CrossRef]

15. Shahid, M.; Farooqi, Z.H.; Begum, R.; Arif, M.; Wu, W.; Irfan, A. Hybrid microgels for catalytic and photocatalytic removal of nitroarenes and organic dyes from aqueous medium: A review. *Crit. Rev. Anal. Chem.* **2020**, *50*, 513–537. [[CrossRef](#)] [[PubMed](#)]
16. Corma, A.; Concepción, P.; Serna, P. A different reaction pathway for the reduction of aromatic nitro compounds on gold catalysts. *Angew. Chem. Int. Ed.* **2007**, *46*, 7266–7269. [[CrossRef](#)]
17. Gupta, V.; Jain, R.; Mittal, A.; Salah şı, T.; Nayak, A. Photo-catalytic degradation of toxic dye amaranth on TiO₂/UV in aqueous suspensions. *Mater. Sci. Eng.* **2012**, *32*, 12–17. [[CrossRef](#)]
18. Vickers, N.J. Animal communication: When i'm calling you, will you answer too? *Curr. Biol.* **2017**, *27*, R713–R715. [[CrossRef](#)]
19. Zhang, J.T.; Wei, G.; Keller, T.F.; Gallagher, H.; Stötzel, C.; Müller, F.A.; Gottschaldt, M.U.; Schubert, K.D. Jandt, Responsive hybrid polymeric/metallic nanoparticles for catalytic applications. *Macromol. Mater. Eng.* **2010**, *295*, 1049–1057. [[CrossRef](#)]
20. Bharech, S.; Kumar, R. A review on the properties and applications of graphene. *J. Mater. Sci. Mech. Eng.* **2015**, *2*, 70.
21. Lee, C.; Wei, X.; Kysar, J.W.; Hone, J. Measurement of the elastic properties and intrinsic strength of monolayer graphene. *Science* **2008**, *321*, 385–388. [[CrossRef](#)]
22. John, R.; Merlin, B. Theoretical investigation of structural, electronic, and mechanical properties of two dimensional C, Si, Ge, Sn. *Cryst. Struct. Theor. Appl.* **2016**, *5*, 43–55. [[CrossRef](#)]
23. Abbott's, I.E. Graphene: Exploring carbon flatland. *Phys. Today* **2007**, *60*, 35.
24. Liu, S.; Liu, C.; Guo, J.; Yan, W. Microstructure and superior electrochemical activity of Cu3P/reduced graphene oxide composite for an anode in lithium-ion batteries. *J. Electrochem. Soc.* **2017**, *164*, A2390. [[CrossRef](#)]
25. Abdi, G.; Alizadeh, A.; Zinadini, S.; Moradi, G. Removal of dye and heavy metal ion using a novel synthetic polyethersulfone nanofiltration membrane modified by magnetic graphene oxide/metformin hybrid. *J. Membr. Sci.* **2018**, *552*, 326–335. [[CrossRef](#)]
26. Chen, D.; Feng, H.; Li, J. Graphene oxide: Preparation, functionalization, and electrochemical applications. *Chem. Rev.* **2012**, *112*, 6027–6053. [[CrossRef](#)]
27. Upadhyay, R.K.; Soin, N.; Roy, S.S. Role of graphene/metal oxide composites as photocatalysts, adsorbents and disinfectants in water treatment: A review. *RSC Adv.* **2014**, *4*, 3823–3851. [[CrossRef](#)]
28. Gong, Z.; Li, S.; Han, W.; Wang, J.; Ma, J.; Zhang, X. Recyclable graphene oxide grafted with poly (N-isopropylacrylamide) and its enhanced selective adsorption for phenols. *Appl. Surf. Sci.* **2016**, *362*, 459–468. [[CrossRef](#)]
29. Ali, S.; Shah, S.J.U.H.; Jamil, S.; Bibi, S.; Shah, M.U.; Aqib, A.I.; Zaheer, T.; Khan, S.R.; Janjua, M.R.S.A. Zirconium nanoparticles-poly (N-isopropylacrylamide-methacrylic acid) hybrid microgels decorated graphene sheets for catalytic reduction of organic pollutants. *Chem. Phys. Lett.* **2021**, *780*, 138915. [[CrossRef](#)]
30. Ashraf, S.; Begum, R.; Rehan, R.; Wu, W.; Farooqi, Z.H. Synthesis and characterization of pH-responsive organic-inorganic hybrid material with excellent catalytic activity. *J. Inorg. Organomet. Polym. Mater.* **2018**, *28*, 1872–1884. [[CrossRef](#)]
31. Farooqi, Z.H.; Khalid, R.; Begum, R.; Farooq, U.; Wu, Q.; Wu, W.; Ajmal, M.; Irfan, A.; Naseem, K. Facile synthesis of silver nanoparticles in a crosslinked polymeric system by in situ reduction method for catalytic reduction of 4-nitroaniline. *Environ. Technol.* **2019**, *40*, 2027–2036. [[CrossRef](#)]
32. Farooqi, Z.H.; Ijaz, A.; Begum, R.; Naseem, K.; Usman, M.; Ajmal, M.; Saeed, U. Synthesis and characterization of inorganic-organic polymer microgels for catalytic reduction of 4-nitroaniline in aqueous medium. *Polym. Compos.* **2018**, *39*, 645–653. [[CrossRef](#)]
33. Farooqi, Z.H.; Naseem, K.; Ijaz, A.; Begum, R. Engineering of silver nanoparticle fabricated poly (N-isopropylacrylamide-co-acrylic acid) microgels for rapid catalytic reduction of nitrobenzene. *J. Polym. Eng.* **2016**, *36*, 87–96. [[CrossRef](#)]
34. Zhang, K.; Suh, J.M.; Choi, J.-W.; Jang, H.W.; Shokouhimehr, M.; Varma, R.S. Recent advances in the nanocatalyst-assisted NaBH₄ reduction of nitroaromatics in water. *ACS Omega* **2019**, *4*, 483–495. [[CrossRef](#)]
35. Lu, Y.; Mei, Y.; Ballauff, M.; Drechsler, M. Thermosensitive core-shell particles as carrier systems for metallic nanoparticles. *J. Phys. Chem. B* **2006**, *110*, 3930–3937. [[CrossRef](#)] [[PubMed](#)]
36. Hussain, I.; Ali, F.; Shahid, M.; Begum, R.; Irfan, A.; Wu, W.; Shaukat, S.; Farooqi, Z.H. Silver nanoparticles supported on smart polymer microgel system for highly proficient catalytic reduction of Cr⁶⁺ to Cr³⁺ with formic acid. *Appl. Organomet. Chem.* **2021**, *35*, e6405. [[CrossRef](#)]
37. Shah, L.A.; Sayed, M.; Fayaz, M.; Bibi, I.; Nawaz, M.; Siddiq, M. Ag-loaded thermo-sensitive composite microgels for enhanced catalytic reduction of methylene blue. *Nanotechnol. Environ. Eng.* **2017**, *2*, 14. [[CrossRef](#)]
38. Khan, S.R.; Farooqi, Z.H.; Ali, A.; Begum, R.; Kanwal, F.; Siddiq, M. Kinetics and mechanism of reduction of nitrobenzene catalyzed by silver-poly (N-isopropylacryl amide-co-allylacetic acid) hybrid microgels. *Mater. Chem. Phys.* **2016**, *171*, 318–327. [[CrossRef](#)]
39. Sargin, I.; Baran, T.; Arslan, G. Environmental remediation by chitosan-carbon nanotube supported palladium nanoparticles: Conversion of toxic nitroarenes into aromatic amines, degradation of dye pollutants and green synthesis of biaryls. *Sep. Purif. Technol.* **2020**, *247*, 116987. [[CrossRef](#)]
40. Albukhari, S.M.; Ismail, M.; Akhtar, K.; Danish, E.Y. Catalytic reduction of nitrophenols and dyes using silver nanoparticles@ cellulose polymer paper for the resolution of waste water treatment challenges. *Colloids Surf. A Physicochem. Eng. Asp.* **2019**, *577*, 548–561. [[CrossRef](#)]
41. Ferraz, E.; de Oliveira, G.; de Oliveira, D.P. The impact of aromatic amines on the environment: Risks and damages. *Front. Biosci.* **2019**, *4*, 914–923. [[CrossRef](#)]

42. Chen, K.; Chen, W.; Yi, X.; Chen, W.; Liu, M.; Wu, H. Sterically hindered *N*-heterocyclic carbene/palladium (ii) catalyzed Suzuki–Miyaura coupling of nitrobenzenes. *Chem. Commun.* **2019**, *55*, 9287–9290. [[CrossRef](#)]
43. Chequer, F.D.; De Oliveira, G.R.; Ferraz, E.A.; Cardoso, J.C.; Zanoni, M.B.; de Oliveira, D.P. Textile dyes: Dyeing process and environmental impact. *Eco-Friendly Text. Dyeing Finish.* **2013**, *6*, 151–176.
44. Varjani, S.; Rakholiya, P.; Ng, H.Y.; You, S.; Teixeira, J.A. Microbial degradation of dyes: An overview. *Bioresour. Technol.* **2020**, *314*, 123728. [[CrossRef](#)]
45. Gürses, A.; Açıkyıldız, M.; Güneş, K.; Gürses, M.S. Dyes and Pigments: Their Structure and Properties. In *Dyes and Pigments*; Springer: Berlin/Heidelberg, Germany, 2016; pp. 13–29.
46. Lin, Y.; Cao, Y.; Yao, Q.; Chai, O.J.H.; Xie, J. Engineering noble metal nanomaterials for pollutant decomposition. *Ind. Eng. Chem. Res.* **2020**, *59*, 20561–20581. [[CrossRef](#)]
47. Din, M.I.; Khalid, R.; Hussain, Z.; Hussain, T.; Mujahid, A.; Najeeb, J.; Izhar, F. Nanocatalytic assemblies for catalytic reduction of nitrophenols: A critical review. *Crit. Rev. Anal. Chem.* **2020**, *50*, 322–338. [[CrossRef](#)]
48. Bibi, G.; Khan, S.R.; Ali, S.; Jamil, S.; Bibi, S.; Shehroz, H.; Janjua, M.R.S.A. Role of capping agent in the synthesis of zinc–cobalt bimetallic nanoparticles and its application as catalyst and fuel additive. *Appl. Nanosci.* **2022**, *12*, 2169–2181. [[CrossRef](#)]
49. UlAin, Q.; Ali, S.; Jamil, S.; Bibi, S.; Khan, S.R.; UrRehman, S.; Bibi, G.; Khan, T.; Shehroz, H.; Hashaam, M. Comparison of catalytic and fuel additive properties of bimetallic nanoparticles and its composite: FeMnO₃ and PANI-FeMnO₃. *Mater. Sci. Semicond. Proc.* **2022**, *144*, 106630. [[CrossRef](#)]
50. Farooqi, Z.H.; Sakhawat, T.; Khan, S.R.; Kanwal, F.; Usman, M.; Begum, R. Synthesis, characterization and fabrication of copper nanoparticles in *N*-isopropylacrylamide based co-polymer microgels for degradation of *p*-nitrophenol. *Mater. Sci. Pol.* **2015**, *33*, 185–192. [[CrossRef](#)]
51. Farooqi, Z.H.; Tariq, N.; Begum, R.; Khan, S.R.; Iqbal, Z.; Khan, A. Fabrication of silver nanoparticles in poly (*N*-isopropylacrylamide-co-allylacetic acid) microgels for catalytic reduction of nitroarenes. *Turk. J. Chem.* **2015**, *39*, 576–588. [[CrossRef](#)]
52. Zubair, N.F.; Jamil, S.; Fatima, S.; Khan, S.R.; Khan, M.U.; Janjua, M.R.S.A. Synthesis of needle like nano composite of rGO-Mn₂O and their applications as photo-catalyst. *Chem. Phys. Lett.* **2020**, *757*, 137874. [[CrossRef](#)]
53. Farooqi, Z.H.; Khan, S.R.; Hussain, T.; Begum, R.; Ejaz, K.; Majeed, S.; Ajmal, M.; Kanwal, F.; Siddiq, M. Effect of crosslinker feed content on catalytic activity of silver nanoparticles fabricated in multiresponsive microgels. *Korean J. Chem. Eng.* **2014**, *31*, 1674–1680. [[CrossRef](#)]